A Simple Minimized Polarization Reconfigurable Slot Antenna

Maziar Hedayati[1], **Mohsen Abdolahi**[1],
Gholamreza Askari[2], **and Hamid Mirmohammad Sadeghi**[2]

[1]Department of Electrical and Computer Engineering
Isfahan University of Technology (IUT), Isfahan 84156, Iran
[2]Information and Communication Technology Institute
Isfahan University of Technology (IUT), Isfahan 84156, Iran

Abstract— Recent developments in the wireless communication industry continue to drive the requirements for small, compatible, and affordable reconfigurable antennas. Polarization-reconfigurable antennas can mitigate multipath fading loss and provide a double-transmission channel for frequency reuse. A polarization-reconfigurable slot antenna, for wireless communication, is presented in this paper. In the proposed design a new shape of slot antenna based on SIW structures at the center frequency 31 GHz is presented which is linear-polarization (LP)/circular-polarization (CP) switchable reconfigurable antenna while the antenna is still operable over the desired frequency band. The proposed antenna is designed and simulated using Ansoft HFSS, a Finite-Element-Method based EM solver. The computed return loss, for each case, is better than 10 dB over the 30–32 GHz frequency range. The 3 dB axial ratio BW around is 11% in the CP state.

1. INTRODUCTION

Wireless communication systems have been developed rapidly in recent years in that systems require an antenna with a wideband, good radiation performances and sometimes switchable ability. To obtain the switchable ability of the antenna, the concept of a reconfigurable antenna was proposed a few years ago [1]. Reconfigurable antennas generally have a frequency, radiation pattern, or polarization tune ability. Frequency, radiation pattern [2–5], and polarization [6–8] reconfigurable antennas are alternatives to broadband/multiband antenna, beam forming array, and dual-polarized antenna, respectively. Polarization-reconfigurable antennas are wireless link terminals that help increase the performance of communications systems through polarization diversity and frequency reuse. But few polarization reconfigurable antennas have recently been presented [9–11]. This is because it's difficult to simultaneously realize a good impedance matching for circular and linear polarizations. In this paper, a very simple polarization-reconfigurable slot antenna, for wireless communication, is proposed.

2. ANTENNA CONFIGURATION AND DESIGN GUIDELINES

The antenna is designed to have the linear and circular polarization. The substrate with $\varepsilon_r = 2.33$, $\tan\delta = 0.0009$, and thickness of 0.508 mm was used for antenna. The design process consists of three parts. At first, designing of single slot then, Calculation of coupling factor and second slot length and finally, reconfigurable antenna design. An overall layout of the designed slots is shown in Fig. 1.

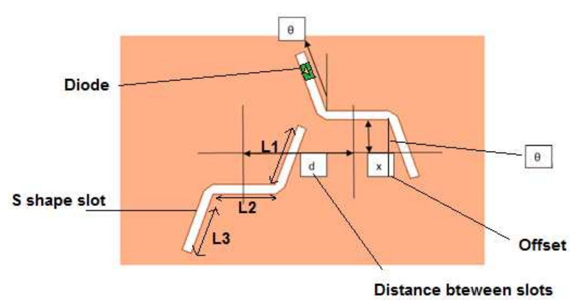

Figure 1: The layout of the designed slot.

2.1.

2.1.1. SIW Design

In the previous years, there have been attempt of different kinds to implement the waveguide in the surface because these elements are cheaper. One of the best method to construct these elements is using the two line of cylindrical conductors that works as a waveguide. The main difference between SIW and conventional waveguide is their propagation modes. In the conventional waveguide all of TM_{nm} and TE_{nm} mode are propagated, but only TE_{n0} is propagated in the SIW. To design of purposed antenna the SIW with $d = 0.8$ mm, $p = 2$ mm, $a = 7.2$ mm, $h = 0.508$ mm, $\varepsilon_r = 2.33$ is used. The cut-off frequency of the SIW is 15.2 GHz that is suitable for the purposed application. All the structures implemented by SIW should be fed accurately. Since dominant modes of rectangular waveguide and microstrip line are similar. A microstrip line is usually used for SIW feeding. The optimized dimensions of feed are $a_1 = 6.096$ mm, $l = 5.588$ mm, $d_1 = 2.286$ mm, $h = 0.508$ mm, $w = 0.711$ mm. Fig. 2 shows surface current of SIW.

2.1.2. Single Slot Design

In an effort to decrease the total area occupied by the antenna, the slot configuration was altered from its standard straight form to an S-shape. From the simulated equivalent magnetic current distribution on the straight and S-shape slots [Fig. 3, antennas (a) and (b)], it is obvious that they both closely follow a sinusoidal pattern with the maximum current concentrated in the middle of the slot. As a result, the two antennas share very similar properties and they only Differ in their polarization orientation.

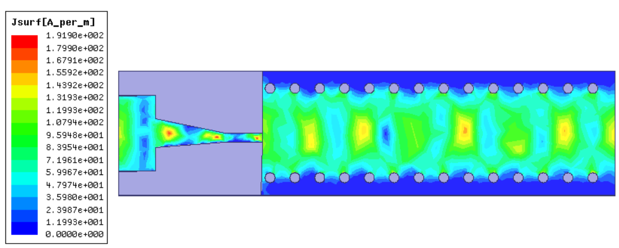

Figure 2: Surface current on SIW.

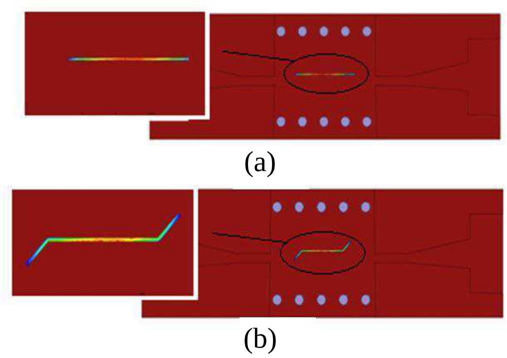

Figure 3: The equivalent magnetic current distribution on the (a) straight and (b) S-shape slots.

Table 1:

	θ	Polarization
1	20	49
2	40	63
3	60	78
4	90	90

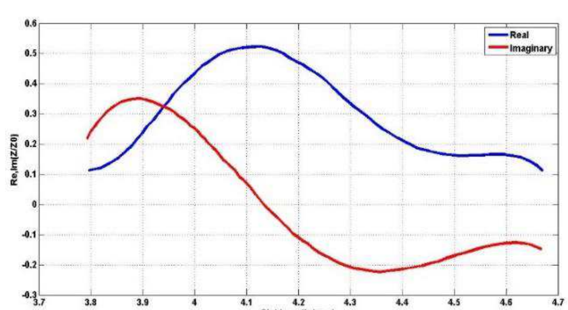

Figure 4: The real and imaginary part of normalized slot impedance vs. length of slot.

Antenna (a) is horizontally polarized, while antenna (b) slant linear polarized. The slot must be placed in a point on SIW surface which the transverse and longitudinal current distribution components of the TE_{10} mode be equal. Two values of x can be found for which $|J_x| = |J_y|$. $x = a/\pi\ (\tan^{-1}(\lambda_g/2a)$ is achieved according to the method that is discussed in [12] which a and λ_g are the width and guided wavelength of SIW, respectively. At the following point, the transverse and longitudinal components of the current distribution are equal in magnitude. If an s-slot be cut at the x point, the produced electric fields in the s-slot branches are equal in magnitude but the transverse and longitudinal components of the electrical field are not exactly the same in s shape slot, so it is necessary to optimize the slot to achieve 45 deg. Polarization which θ in Fig. 1 must be $20°$ and $\frac{L_1+L_3}{L_2} < 0.37$. Table 1 shows the effect of θ vs. polarization. HFSS software is used to simulate an isolated S shape slot to achieve its length according to the method in [13]. Fig. 4 shows the real and imaginary part of normalized slot impedance vs. length of slot. So the length of slot is obtained 4.12 mm for first slot.

2.2. Calculation of Coupling Factor

By means of the model in Fig. 5, the coupling coefficient, indicating the amount of radiation from a single slot is derived. The slot is placed in its calculated offset from previous section and the length of module is $\lambda_g/2$.

The reference planes at two ports should be shifted inward to remove the transmission line effects. This yields

$$S = \begin{pmatrix} S_{11} & S_{12} \\ S_{21} & S_{22} \end{pmatrix}$$
$$S = \begin{pmatrix} e^{2j\beta 10s} & 0 \\ 0 & e^{2j\beta 10s} \end{pmatrix} S^b \begin{pmatrix} e^{2j\beta 10s} & 0 \\ 0 & e^{2j\beta 10s} \end{pmatrix}$$

where S^b is the scattering parameters matrix calculated by the simulation software and β_{10} is the propagation constant for TE_{10} mode.

S matrix of calculated slot is shown in Fig. 7. So coupling factor is obtained as follow $|S_{21}|^2 + |S_{11}|^2 + |S_{31}|^2 = 1$, $|S_{21}| = 0.8$, $|S_{11}| = 0.079$, $|S_{31}| = \alpha = 0.59|S_{21}| = 0.8$ must be applied to the

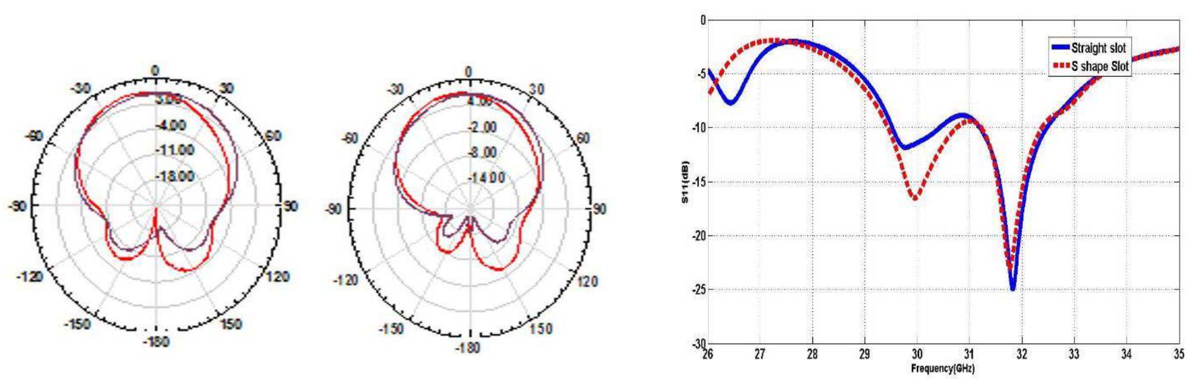

(a) (b)

Figure 5: (a) The pattern and (b) the S parameter of straight and S-shape slot.

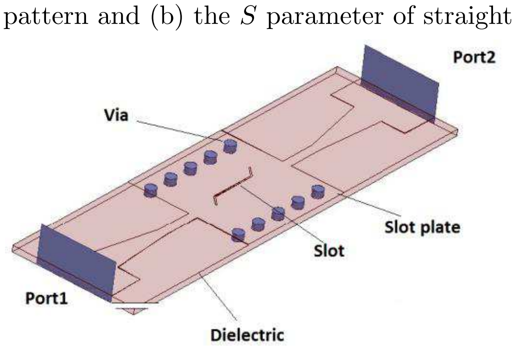

Figure 6: Structure model to calculate coupling.

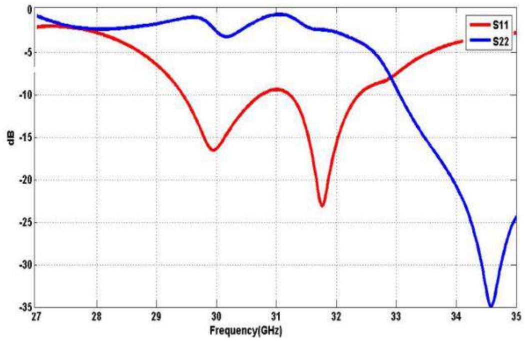

Figure 7: The S matrix of calculated slot.

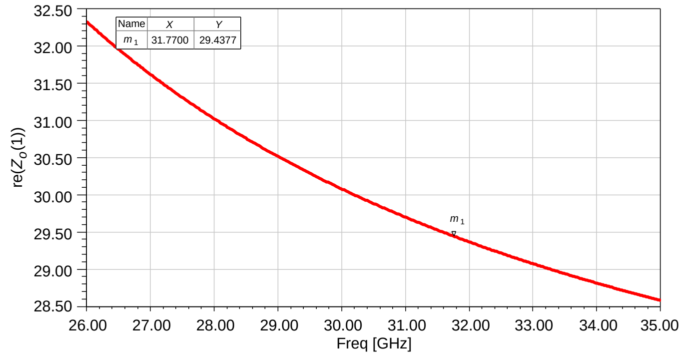

Figure 8: The input impedance of first module.

input of second slot to achieve the second slot length to have the same coupling coefficient. But the input impedance of second module is not 50 anymore. So output of first module should be applied to output of second module. Fig. 8 shows the input impedance of first module which is 29 Ω at 32 GHz. With this scenario the length of second slot is obtained 4.32 mm. So all of necessary parameters to design the antenna in Fig. 1 are obtained.

2.3. Reconfigurable Antenna Design and Simulation Result

There are various elements and techniques implemented in order to achieve the tune ability: micro electromechanical switches (MEMS), varactors, PIN diodes, FET transistors, and special substrate materials like ferroelectric or ferromagnetic materials. In this paper PIN diodes are used, because PIN diode's reliability, compact size, high switching speed, small resistance and capacitance in the ON and OFF state, respectively, make it most appropriate for the application at hand. But at first a biased circuit must be intruded for diode. The switch bias network is presented in Fig. 9. An inductor is necessary for RF signal isolation but lumped elements do not have appropriate behavior in high frequencies because their self-resonance frequency is less than 31 GHz. The Stub is designed

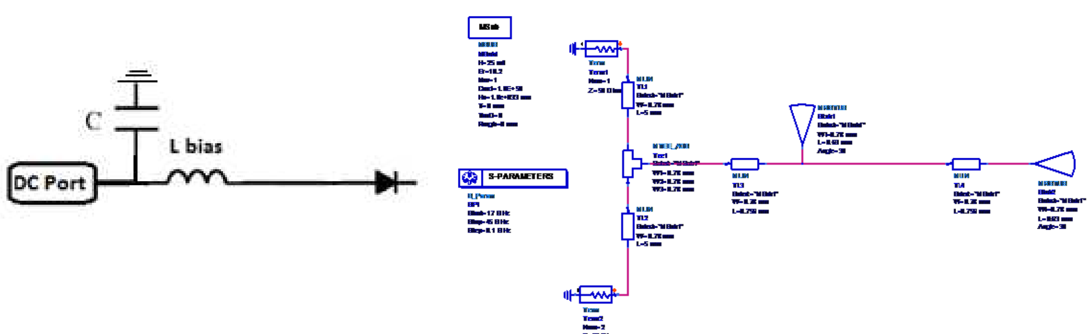

Figure 9: The biased circuit for diode.

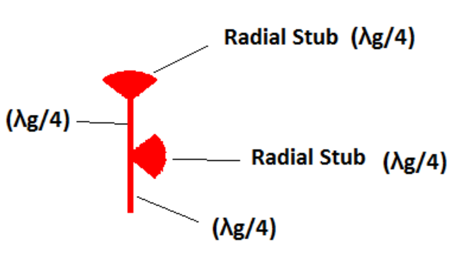

Figure 10: The stub is designed by two $\lambda_g/4$ open circuit radial stub line.

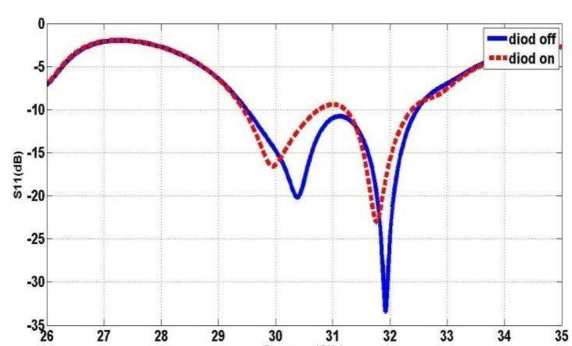

Figure 11: The S parameter of antenna.

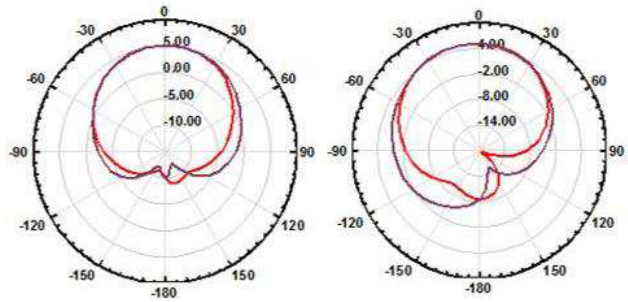

Figure 12: The computed radiation patterns, in the X-Z and Y-Z planes, at 31 GHz for diode on and off.

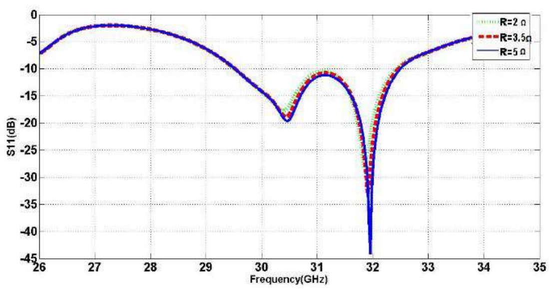

Figure 13: The simulated return loss versus the switch ON state resistance for three different cases between 2 to 5 Ω.

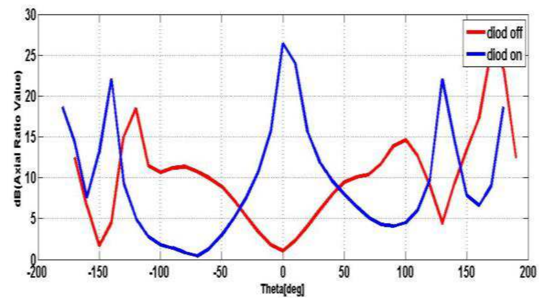

Figure 14: The axial-ratio of the proposed antenna.

by two $\lambda_g/4$ open circuit radial stub line which enhance stub bandwidth (Fig. 10). Furthermore two 2.7 pF capacitors are used to improve the DC isolation. The diode is placed on slot and its bias circuit is on a separate substrate which is connected to diode with appropriate wires. The antenna was designed and simulated using Ansoft HFSS for one switching conditions. Computed return loss plots, as depicted in Fig. 11 shows that the antenna operate in 30–32 GHz in both case (diode on and off). The return loss is acceptable in both case and there is not necessary any additional switch to tune the resonance frequency. The computed radiation patterns, in the X-Z and Y-Z planes, at 31 GHz for diode on and off, are shown in Fig. 12. The small ON state resistance also affects the Antenna performance and particularly its input impedance. Full wave analysis was used to model these effects. For a first order approximation, the diode resistance was modeled as a thin film resistor on top of the slot and the packaging parasitic elements were neglected in this analysis. Fig. 13 shows the simulated return loss versus the switch ON state resistance for three different cases between 2 to 5 Ω. As it is shown in this figure, the parasite resistance does not effect on antenna performances. The radiation of the antenna is acceptably the same. However, the efficiency and the gain will be reduced compared to a half-wavelength slot due to the resistive losses caused by the diodes. When diode is on, the gain of antenna is 0.5 dB less than another one and the side lobe level is more than when diode is off. But In either case, the antenna is expected to have maximum radiation in $\theta = 0$. Accordingly, the axial-ratio of the proposed antenna is shown in Fig. 14. As it is shown in this figure when diode is off the ratio of E_x and E_y is one with 90° differences in phase but when diode is on, this ratio is not one anymore, so there is not circular polarization anymore.

ACKNOWLEDGMENT

The authors would like to thank ICTI (Information and communication technology institute) to support of this project.

REFERENCES

1. Peroulis, D., K. Sarabandi, and L. P. B. Katehi, "A planar VHF reconfigurable slot antenna," *IEEE Antennas and Propagation Society International Symposium*, Vol. 1, 154–157, Jul. 8–13, 2001.

2. Chen, S.-H., J.-S. Row, and K.-L. Wong, "Reconfigurable square-ring patch antenna with pattern diversity," *IEEE Trans. Antennas Propag.*, Vol. 55, No. 2, 472–475, Feb. 2007.
3. Wu, S.-J. and T.-G. Ma, "A wideband slotted bow-tie antenna with reconfigurable CPW-to-slot line transition for pattern diversity," *IEEE Trans. Antennas Propag.*, Vol. 56, No. 2, 327–334, Feb. 2008.
4. Huff, G. H. and J. T. Bernhard, "Integration of packaged RF MEMSS witches with radiation-pattern-reconfigurable square spiral microstrip Antennas," *IEEE Trans. Antennas Propag.*, Vol. 54, No. 2, 464–469, Feb. 2006.
5. Jung, C. W., M. J. Lee, G. Li, and F. de Flaviis, "Reconfigurable scan beam single-arm spiral antenna integrated with RF-MEMS switches," *IEEE Trans. Antennas Propag.*, Vol. 54, No. 2, 455–463, Feb. 2006.
6. Sung, Y., "Investigation into the polarization of asymmetrical-feed triangular microstrip antennas and its application to reconfigurable antennas," *IEEE Trans. Antennas Propag.*, Vol. 58, No. 4, 1039–1046, Apr. 2010.
7. Simons, R. N., D. Chun, and L. P. B. Katehi, "Polarization-reconfigurable patch antenna using microelectromechanical-system (MEMS) actuators," *IEEE Antennas Propag. Soc. Int.*, Vol. 2, 6–9, 2002.
8. Yang, F. and Y. Rahmat-Samii, "A reconfigurable patch antenna using switchable slots for circular polarization diversity," *IEEE Microw. Wireless Compon. Lett.*, Vol. 12, No. 3, 96–98, Mar. 2002.
9. Qin, P.-Y., A. R. Weily, Y. J. Guo, and C.-H. Liang, "Polarization reconfigurable U-slot patch antenna," *IEEE Trans. Antennas Propag.*, Vol. 58, 3383–3388, Oct. 2010.
10. Parihar, M. S., A. Basu, and S. K. Koul, "Polarization reconfigurable microstrip antenna," *Proceedings of the Asia-Pacific Microwave Conference, APMC'09*, 1918–1921, Singapore, 2009.
11. Monti, G., L. Corchia, and L. Tarricone, "Patch antenna with reconfigurable polarization," *Progress In Electromagnetics Research*, Vol. 9, 13–23, 2009.
12. Simmons, A. J., "Circularly polarized slot radiators," *IRE Transactions on Antennas and Propagation*, Vol. 5, No. 1, 31–36, Jan. 1957.
13. Oraizi, H. and M. T. Noghani, "Design and optimization of waveguide fed centered inclined slot arrays," *IEEE Trans. Antennas Propag.*, Vol. 57, No. 12, 3993–3997, Dec. 2009.